Table 6. Activation of CD8-depleted peripheral-blood mononuclear cells by a combination of anti-CD3 and interleukin-2.

The table is available in its entirety in the online edition of the *Journal of Infectious Diseases*.

not only at a single time point but throughout the sampling period. For example, integrations into position 90819497 on chromosome 6 were independently identified by PCR in samples from 1998, 2000, 2002 (twice), and 2004. The identical integration sites that were observed in the *BACH2* gene of patient 1 were found for other genes in this patient, as well as in other patients. This finding, summarized in table 5, indicates that HIV-1–infected cells persist for long periods and may undergo clonal expansion. Collectively, our data show that, for patient 1, HIV-1 preferred to integrate within the *BACH2* locus, and, despite the reduction in pDNA level, cells carrying HIV-1 integrated into the *BACH2* gene were maintained during longitudinal HAART.

Integration of HIV-1 into genes that are actively transcribed in resting CD4⁺ T cells. It was recently reported that, even in resting CD4⁺ T cells, HIV-1 genomes reside in vivo predominantly in host genes that are actively transcribed [21]. To examine whether this finding is also true of host genes identified in the present study, the expression of the targeted genes in activated and resting CD4⁺ T cells were examined by RT-PCR. Eighteen genes among all transcriptional units in which an integration site was identified were analyzed. Using *HLA-DR* as a marker for activation (figure 3*A*), we found that the mRNA for all 18 genes was clearly detectable in both activated and resting CD4⁺ T cells from a seronegative donor (figure 3*B* and data not shown). The *BACH2* gene was also actively transcribed in resting CD4⁺ T cells from seronegative donors and, importantly, from patient 1 as well (figure 3*C* and 3*D*). Thus, the HIV-1 genomes appear to reside predominantly in genes that are actively transcribed in resting CD4⁺ T cells, consistent with a recent report [21].

In resting CD4⁺ T cells, the majority of integrated HIV-1 DNA is present in cells of the memory subset [1, 12]. We therefore investigated whether resting and resting memory CD4⁺ T cells express similar genes. For all genes examined, the memory subset of resting CD4⁺ T cells was shown to have an expression pattern that is very similar to that of the entire resting CD4⁺ T cell population (figure 3*B* and 3*C*).

Failure of activation stimuli to reactivate HIV-1 in patient 1, who had an integration cluster on the* BACH2 *gene. Several studies have demonstrated the presence of replication-competent virus in patients whose plasma viremia decreased to below detectable levels while receiving HAART [2–4, 6, 8, 9, 11, 12]. We therefore examined the transcription of residual HIV-1 DNA in PBMCs from our patients. As shown in table 6, there were measurable amounts of p24 antigens in culture supernatants of PBMCs from patients with viremia 1 and 2 and the 3 patients without viremia earlier during the clinical course, indicating that the assays are capable of recovering antigen even from the samples from the patients with viremia. In contrast, p24 antigen was consistently undetectable in CD8-depleted PBMCs from patients 1 and 2.

In parallel, we also performed an RT-PCR assay to analyze HIV-1 transcription in CD8-depleted PBMCs from patients 1 and 2 after activation. As shown in figure 4, MS, SS, and US mRNAs were detected in cells from patients with viremia 1 and 2, as well as in JR-FL–infected PM1 cells. In contrast, no mRNA species were detected in patient 1 with integration clusters in the *BACH2* gene. Interestingly, although MS and SS bands were detected in patient 2 by the RT-PCR assay, the US band was not. These results may reflect the fact that much of pDNA is defective and, in patients receiving long-term HAART, only a

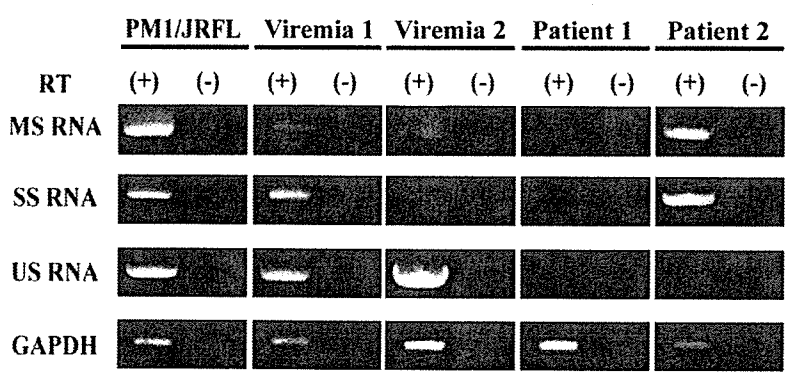

Figure 4. Characterization of CD8-depleted peripheral-blood mononuclear cells (PBMCs) from patients without viremia receiving highly active antiretroviral therapy and detection of multiply spliced (MS), singly spliced (SS), and unspliced (US) HIV-1 RNA in CD8-depleted PBMCs by reverse-transcriptase polymerase chain reaction (RT-PCR). CD8-depleted PBMCs were cultured with anti-CD3 and interleukin-2 for 7 days. PBMCs from patients with viremia (viremia 1 and 2) were used as positive controls for RT-PCR.

Table 7. Characteristics of integration sites identified from HIV-1–infected individuals in the present study.

The table is available in its entirety in the online edition of the *Journal of Infectious Diseases*.

fraction of $CD4^+$ T cells contains a provirus capable of high-level HIV-1 gene expression after activation [6, 12].

DISCUSSION

In the present study, the integration sites in residual HIV-1 in patients with prolonged viral suppression by HAART were investigated. Consistent with results from recent genomewide in vitro [16, 30] and in vivo [21] studies, we found that most integration events occur in introns within transcriptional units of the host genome. Many of the genes found to carry HIV-1 integration sites were actively expressed in circulating resting $CD4^+$ T cells from seronegative donors. Nevertheless, low-frequency integrations into the alphoid-repeat regions of centromeres were also observed [16, 18, 19], suggesting that integration into heterochromatin regions may play a minor role in viral latency in vivo. Considering that the majority of proviruses have a replication-defective phenotype, it is possible that a minor population of viruses integrated into chromosomal regions where transcription is repressed may harbor a replication-competent phenotype.

The sequences of several thousand retroviral integration sites have been reported. Most were obtained from analysis of infected T cell lines or T cells transduced with HIV-1 vectors [16, 30]. Because of the activated and proliferating nature of these infected or transduced cells, the findings in these tissue culture cell systems may not be relevant to the environment of latently infected cells in vivo. In this regard, we found that short interspersed nuclear elements containing *Alu* sequences were favored for integration during the course of HIV infection under HAART, a result that is consistent with the findings of previous studies of HIV integration sites during productive infection of cultured cells [16, 28, 30]. On the other hand, ~8% of the human genome is composed of >230,000 endogenous retroviruses (HERVs), but HIV integration in vivo is found to be strongly disfavored in these LTR elements. Intriguingly, integration into the *STAT5B* gene, which regulates cell proliferation, differentiation, and survival [31], was found in 4 of 7 patients (table 7). It appears to be possible that rare integrations into such sites, which involve cell proliferation, occur in vivo and that such integrations are associated with clonal expansion of infected cell populations. On the other hand, because the analyses in this study were done with bulk and not purified resting $CD4^+$ T cells, it is conceivable that these integration events are present in small populations of proliferating T cells within the bulk preparation.

Of interest, however, is our data demonstrating a remarkable cluster for HIV-1 integration in the *BACH2* gene. Furthermore, in contrast to HERVs, which integrate in the reverse direction of cellular gene transcription [32], the transcriptional orientation of integrated HIV-1 genomes and the *BACH2* gene is the same (figure 2*A*). Clonal expansion of infected cell populations cannot fully explain the unique clustering of HIV-1 integration into the *BACH2* gene locus observed in patients 1 and 3, raising the possibility of the existence of some host machinery that actively directs the HIV-1 preintegration complex (PIC) to their DNA target location. Furthermore, target-site selection of HIV-1 integration appears to be influenced by transcriptional activity [28]. *BACH2* is abundantly expressed in B lymphocytes as well as lymphoma cell lines of B cell origin and plays roles in the regulation of B cell development [33]. It is also expressed in T lymphoid cell lines [33, 34], although the function of this transcription factor in T lymphocytes is unknown. We have shown, by RT-PCR, that *BACH2* mRNA was also expressed in resting $CD4^+$ T cells from seronegative donors as well as from patient 1 (figure 3). Our findings reveal unexpected specificity in integration targeting by HIV-1. The molecular mechanism for this strong favoring remains to be elucidated, but such bias toward the integration site in vivo may be driven by an association between PIC and host cell proteins. Identification of host cell factors that control the selection of integration sites should reveal new targets for antiretroviral drugs.

It is generally accepted that, despite the presence of integrated HIV-1 DNA, there is no detectable virus production in cultured resting $CD4^+$ T cells from patients receiving HAART without some cellular activation in vitro [2, 3, 6, 14]. The basis for the nonproductive nature of the infection in resting $CD4^+$ T cells with integrated HIV-1 DNA appears to be multiple. Besides the chromatin environment at the site of integration, resting $CD4^+$ T cells may harbor defective HIV-1 genomes. In addition, it has been shown that HIV-1 mRNA, especially US mRNA, is synthesized quite inefficiently in latently infected resting $CD4^+$ T cells from patients receiving suppressive HAART, possibly reflecting regulation at the level of mRNA production [6]. We found that virion release was undetectable after ex vivo stimulation of CD8-depleted PBMCs from 2 patients without viremia who were receiving HAART (table 6). Furthermore, RT-PCR demonstrated that SS or MS, but not US, HIV-1 mRNAs were present in patient 2 but were below the limit of detection in the other 3 patients (figure 4 and data not shown). Thus, the nonproductive nature of the infection in resting $CD4^+$ T cells must be caused by mechanisms unrelated to the nature of the integration site.

In summary, we have shown that HIV-1 integrates in intronic

regions of actively transcribed genes in vivo. A certain degree of target-site selectivity for HIV-1 integration was also observed. The relationships between integration, latent infection, and host cell factors merit further investigation.

Acknowledgments

We are grateful to Cecilia Cheng-Mayer, for critically reviewing the manuscript. We also thank Kazuhiko Igarashi, for valuable information; Tetsuya Kimura, for discussions; and Yuki Azakami and Akiko Honda, for help in sequencing.

References

1. Brenchley JM, Hill BJ, Ambrozak DR, et al. T-cell subset that harbor human immunodeficiency virus (HIV) in vivo: implications for HIV pathogenesis. J Virol **2004**; 78:1160–8.
2. Chun TW, Stuyver L, Mizell SB, et al. Presence of an inducible HIV-1 latent reservoir during highly active antiretroviral therapy. Proc Natl Acad Sci USA **1997**; 94:13193–7.
3. Chun TW, Justement JS, Lempicki RA, et al. Gene expression and viral production in latently infected, resting CD4$^+$ T cells in viremic versus aviremic HIV-infected individuals. Proc Natl Acad Sci USA **2003**; 100: 1908–13.
4. Finzi D, Hermankova M, Pierson T, et al. Identification of a reservoir for HIV-1 in patients on highly active antiretroviral therapy. Science **1997**; 278:1295–300.
5. Finzi D, Blankson J, Siliciano JD, et al. Latent infection of CD4$^+$ T cells provides a mechanism for lifelong persistence of HIV-1, even in patients on effective combination therapy. Nat Med **1999**; 5:512–7.
6. Hermankova M, Siliciano JD, Zhou Y, et al. Analysis of human immunodeficiency virus type 1 gene expression in latently infected resting CD4$^+$ T lymphocytes in vivo. J Virol **2003**; 77:7383–92.
7. Lassen KG, Bailey JR, Siliciano RF. Analysis of human immunodeficiency virus type 1 transcriptional elongation in resting CD4$^+$ T cells in vivo. J Virol **2004**; 78:9105–14.
8. Lassen K, Han Y, Zhou Y, Siliciano J, Siliciano RF. The multifactorial nature of HIV-1 latency. Trends Mol Med **2004**; 10:525–31.
9. Ramrantnam B, Mittler JE, Zhang L, et al. The decay of the latent reservoir of replication-competent HIV-1 is inversely correlated with the extent of residual viral replication during prolonged anti-retroviral therapy. Nat Med **2000**; 6:82–5.
10. Siliciano JD, Kajdas J, Finzi D, et al. Long-term follow-up studies confirm the stability of the latent reservoir for HIV-1 in resting CD4$^+$ T cells. Nat Med **2003**; 9:727–8.
11. Wong JK, Hezareh M, Günthard HF, et al. Recovery of replication-competent HIV despite prolonged suppression of plasma viremia. Science **1997**; 278:1291–5.
12. Chun TW, Carruth L, Finzi D, et al. Quantification of latent tissue reservoirs and total body viral load in HIV-1 infection. Nature **1997**; 387:183–8.
13. Pierson TC, Zhou Y, Kieffer TL, Ruff CT, Buck C, Siliciano RF. Molecular characterization of preintegration latency in human immunodeficiency virus type 1 infection. J Virol **2002**; 76:8518–31.
14. Chun TW, Finzi D, Margolick J, Chadwick K, Schwartz D, Siliciano RF. In vivo fate of HIV-1-infected T cells: quantitative analysis of the transition to stable latency. Nat Med **1995**; 1:1284–91.
15. Persaud D, Zhou Y, Siliciano JM, Siliciano RF. Latency in human immunodeficiency virus type 1 infection: no easy answers. J Virol **2003**; 77:1659–65.
16. Schröder AR, Shinn P, Chen H, Berry C, Ecker JR, Bushman F. HIV-1 integration in the human genome favors active genes and local hotspots. Cell **2002**; 110:521–9.
17. Jordan A, Defechereux P, Verdin E. The site of HIV-1 integration in the human genome determines basal transcriptional activity and response to Tat transactivation. EMBO J **2001**; 20:1726–38.
18. Jordan A, Bisgrove D, Verdin E. HIV reproducibly establishes a latent infection acute infection of T cells in vitro. EMBO J **2003**; 22:1868–77.
19. Lewinski MK, Bisgrove D, Shinn P, et al. Genome-wide analysis of chromosomal features repressing human immunodeficiency virus transcription. J Virol **2005**; 79:6610–9.
20. Weinberger LS, Burnett JC, Toettchcer JE, Arkin AP, Schaffer DV. Stochastic gene expression in a lentiviral positive-feedback loop: HIV-1 tat fluctuations drive phenotypic diversity. Cell **2005**; 122:169–82.
21. Han Y, Lassen K, Monie D, et al. Resting CD4$^+$ T cells from human immunodeficiency virus type 1 (HIV-1)-infected individuals carry integrated HIV-1 genomes within actively transcribed host genes. J Virol **2004**; 78:6122–33.
22. Douek DC, Brenchley JM, Betts MR, et al. HIV preferentially infects HIV-specific CD4+ T cells. Nature **2002**; 417:95–8.
23. Kuiken CL, Foley B, Hahn B, et al. HIV sequence compendium 2001. Los Alamos, NM: Theoretical Biology and Biophysics Group, Los Alamos National Laboratory, **2001**.
24. Wang FX, Xu Y, Sullivan J, Souder E, et al. IL-7 is a potent and proviral strain-specific inducer of latent HIV-1 cellular reservoirs of infected individuals on virally suppressive HAART. J Clin Invest **2005**; 115:128–37.
25. Maglott DR, Katz KS, Sicotte H, Pruitt KD. NCBI's LocusLink and RefSeq. Nucleic Acids Res **2000**; 28:126–8.
26. Lander ES, Linton LM, Birren B, et al. Initial sequencing and analysis of the human genome. Nature **2001**; 409:860–921.
27. Bushman F, Lewinski M, Ciuffi A, et al. Genome-wide analysis of retroviral DNA integration. Nat Rev Microbiol **2005**; 3:848–58.
28. Mitchell RS, Beitzel BF, Schröder AR, et al. Retroviral DNA integration: ASLV, HIV, and MLV show distinct target site preferences. PLoS Biol **2004**; 2:e234.
29. Mungall AJ, Palmer SA, Sims SK, et al. The DNA sequence and analysis of human chromosome 6. Nature **2003**; 425:805–11.
30. Wu X, Li Y, Crise B, Burgess SM. Transcription start regions in the human genome are favored targets for MLV integration. Science **2003**; 300:1749–51.
31. Hendry L, John S. Regulation of STAT signaling by proteolytic processing. Eur J Biochem **2004**; 271:4613–20.
32. Smit AF. Interspersed repeats and other momentos of transposable elements in mammalian genomes. Curr Opin Genet Dev **1999**; 9:657–63.
33. Sasaki S, Ito E, Toki T, et al. Cloning and expression of human B cell-specific transcription factor *BACH2* mapped to chromosome 6q15. Oncogene **2000**; 19:3739–49.
34. Vieira SA, Deininger MW, Sorour A, et al. Transcription factor *BACH2* is transcriptionally regulated by the BCR/ABL oncogene. Genes Chromosomes Cancer **2001**; 32:353–63.

JVI Accepts, published online ahead of print on 24 January 2007
J. Virol. doi:10.1128/JVI.01544-06
Copyright © 2007, American Society for Microbiology and/or the Listed Authors/Institutions. All Rights Reserved.

Impact of V2 mutations for escape from a potent neutralizing anti-V3 monoclonal antibody during in vitro selection of a primary HIV-1 isolate

Junji Shibata[1], Kazuhisa Yoshimura[1], Akiko Honda[1], Atsushi Koito[1], Toshio Murakami[2] and Shuzo Matsushita[1*]

Division of Clinical Retrovirology and Infectious Diseases, Center for AIDS Research, Kumamoto University, Kumamoto 860-0811[1], and The Chemo-Sero-Therapeutic Research Institute, Kyokushi, Kikuchi, Kumamoto 869-1298, Japan[2]

Running title: Anti-V3 MAb escape variant with V2 mutations

Word count; abstract: 247, text: 6763

*Correspondence should be addressed to: S. M.

Postal address: Shuzo Matsushita MD PhD
Division of Clinical Retrovirology and Infectious Diseases, Center for AIDS Research, Kumamoto University, Kumamoto 860-0811, Japan
Phone: +81-96-373-6536
Facsimile: +81-96-373-6537

e-mail: shuzo@kaiju.medic.kumamoto-u.ac.jp

*This work was presented in part at the 13th Conference on Retroviruses and Opportunistic Infection, Denver, CO, USA, February 5-8, 2006 [Abstract no. 415].

Abstract

KD-247, a humanized monoclonal antibody (MAb) to an epitope of gp120-V3-tip, has potent cross-neutralizing activity against subtype B primary human immunodeficiency virus type 1 (HIV-1) isolates. To assess how KD-247 escape mutants can be generated, we induced escape variants by exposing bulked primary R5 virus, MOKW, to increasing concentrations of KD-247 in vitro. In the presence of relatively low concentrations of KD-247, viruses with two amino acid (aa) mutations (R166K/D167N) in V2 expanded, and under high KD-247 pressure, a V3-tip substitution (P313L) emerged in addition to the V2 mutations. However, a virus with a V2 175P mutation dominated during passaging in the absence of KD-247. Using domain swapping analysis, we demonstrated that the V2 mutations and the P313L mutation in V3 contribute to partial and complete resistant phenotypes against KD-247, respectively. To identify the V2 mutation responsible for the resistance to KD-247, we constructed pseudoviruses with single or double aa mutations in V2 and measured their sensitivity to neutralization. Interestingly, the neutralization phenotypes were switched, so that the 175th aa (Pro or Leu) located in the center of V2 was exchanged, indicating that the 175th aa has a crucial role; dramatically changing the Env oligomeric state on the membrane surface and affecting the neutralization phenotype against not only anti-V3 antibody but also rsCD4. These data suggested that HIV-1 can escape from anti-V3 antibody attack by changing the conformation of the functional envelope oligomer by acquiring mutations in the V2 region in environments with relatively low antibody concentrations.

Introduction

The envelope protein (Env) of human immunodeficiency virus type-1 (HIV-1) presents on the virus surface as 'spikes' composed of trimers comprising three gp120-gp41 complexes (6, 32, 33). Among the regions that induce the neutralization antibody (NAb) response, the third variable domain (V3 loop) of gp120 is considered one of the major targets of the host immune response (23, 69). It has been estimated that as much as half the antibody response against HIV-1 Env in patient sera is directed against the V3 region (43). A recent crystallographic study revealed that the V3 loop contains features that are essential for coreceptor binding and that the extended nature and antibody accessibility of V3 is associated with its immunodominance (20).

HIV-1 primary isolates are relatively resistant to neutralization by NAb and recombinant soluble CD4 (rsCD4) compared with variants selected for growth in permanent cell lines (42, 52, 55). Studies addressing differences between neutralization-sensitive and -resistant variants have revealed the involvement of several mechanisms that underlie the neutralization resistance of primary isolates, including the occlusion of epitopes within the oligomer, extensive glycosylation and extension of variable loops from the surface of the complex, as well as steric and conformational blocking of receptor binding sites (7, 12, 32, 38, 49, 50, 54, 62). The structural features of gp120 tolerate a vast array of mutations that permit the selection of neutralization escape variants, as has been previously demonstrated in culture assays, animal models and infected individuals (24).

Although there is ample data showing that NAb can protect against HIV-1 infection in vitro and in animal models in vivo, activity in infected humans remains

controversial (3, 4, 9, 14, 22, 40, 48, 58). Studies addressing NAb in primary infections have suggested that most recently infected individuals mount a vigorous antibody response against autologous viruses. However, the rapid evolution of HIV in the presence of NAb results in the emergence of escape mutants. As a consequence, at any time during an early stage of the HIV disease, NAb are more likely to recognize earlier autologous viruses than contemporaneous ones. Despite evidence of phenotypic resistance, the genetic basis of the mechanism allowing primary viruses to escape from NAb is poorly understood. Wei et al. found that glycosylation in the envelope plays an important role in allowing escape from neutralization (62). In contrast, in a recent study Frost et al. found that viral escape from NAb is correlated with the rate of amino acid substitution rather than changes in glycosylation or insertions or deletions in the envelope (14). Because of the polyclonal nature of NAb in patient sera, it is difficult to clarify the genetic mechanism responsible for neutralization escape.

Neutralization escape from anti-V3 monoclonal antibodies (MAbs) has been induced in TCLA viruses in several experiments, and associated with amino acid substitution within the epitope in the V3 loop (8, 37, 65). However, Park et al. showed that human sera with neutralizing antibodies, which contained polyclonal antibodies directed at the V3 region, induced neutralization-resistant variants without V3 amino acid substitution (46). Neutralization studies using anti-V3 antibodies against primary isolates suggest that the neutralization-resistant phenotype is associated with changes in the sequences outside V3, rather than variation within the V3 epitope (29, 62). However, the contribution of each change in the envelope to the emergence of escape mutants remains unclear because they are not selected under neutralizing MAbs pressure.

Recently, we described a humanized MAb, KD-247 that displayed cross-neutralizing activity against HIV-1 clade B isolates (11). The epitope of KD-247 was mapped to six amino acids around the PGR core sequence at the tip of the V3 loop. The shortest reactive peptide recognized by KD-247 was determined to be IGPGR, which is shared by 49% of HIV-1 isolates in clade B (35). As well, complete protection from challenge infection by a pathogenic strain of $SHIV_{89.6}$ was observed when using a high concentration of the antibody in an animal model (10). A molecularly cloned CCR5-tropic HIV-1 strain, JR-FL, which is relatively resistant to neutralization (15, 50), was exposed to KD-247 to obtain a neutralization-escape mutant (67). Induction of the neutralization-resistant virus with a mutation in the V3-tip was observed in the presence of a high concentration of KD-247 and the escape variant was found to be more sensitive to CCR5 inhibitors and rsCD4 than the original strain (67).

The present study sought to understand how virus mutation impacts on the activity of an anti-V3 MAb, KD-247. For this we subjected a primary R5 virus, MOKW, to selection pressure by KD-247. The present data suggested that it is necessary to pass a phased step so that the escape mutant against the anti-V3 antibody can emerge. Neutralization escape variants with V2 mutations in gp120 could be selected at relatively low KD-247 pressures, but high concentrations of KD-247 were required for induction of a completely resistant variant with amino acid substitution in the epitope. Moreover, we present evidence suggesting that some V2 mutations change the tertiary or quaternary structure of the envelope trimers on the viral surface that are involved in the neutralization resistance of the primary isolate. Clarification of the mechanisms responsible for this neutralization resistance may provide important insight into possible methods for the

induction of potent and cross-neutralizing antibody responses capable of neutralizing various primary isolates.

ACCEPTED

Materials & Methods

Cells, culture conditions, reagents and viruses. PM1/CCR5 cells (68) were maintained in RPMI-1640 (Sigma) supplemented with 10% heat-inactivated calf serum (FCS: HyClone Laboratories, Logan, UT), 50 U/ml of penicillin, 50 mg/ml of streptomycin and 100 μg/ml of G418 (Sigma). 293T cells were maintained in Dulbecco's modified Eagle medium (DMEM; Sigma) supplemented with 10% heat-inactivated FCS. The CD4- and CCR5-expressing human osteogenic sarcoma cell line GHOST-hi5 was maintained in DMEM supplemented with 10% FCS, G418 (200 μg/ml), hygromycin B (100 μg/ml; Sigma) and puromycin (1 μg/ml; Sigma).

KD-247, an anti-gp120-V3 antibody, was produced as previously described (11). 17b, a monoclonal antibody against the CD4-induced epitope and IgGb12, a monoclonal antibody against the CD4-binding epitope were provided by the National Institutes of Health AIDS Research and Reference Reagent Program. 447-52D, an anti-gp120 V3 MAb, was gift from Dr. Suzan Zolla-Pazner (New York University School of Medicine). 2D7, an anti-CCR5 MAb, and RPA-T4, an anti-CD4 MAb, were purchased from BD Biosciences Pharmingen (San Jose, CA, USA). Recombinant human soluble CD4 (rsCD4) was purchased from R&D systems, Inc. (Minneapolis, MN). TAK-779, a CCR5 inhibitor, was kindly provided by Takeda Chemical Industries Ltd. (Osaka, Japan). AK-602, a CCR5 inhibitor, was gifted by Ono Pharmaceutical Co. Ltd., Osaka, Japan.

The R5 primary HIV-1, MOKW, was isolated from a drug-naïve Japanese patient (36). This virus was passaged in phytohemagglutinin (PHA)-activated peripheral blood mononuclear cells (PBMCs) and the culture supernatant stored at -80°C until use.

Isolation of a KD-247-resistant mutant from MOKW in vitro. The selection of KD-247 escape variants from MOKW was performed as previously described (67). Briefly, MOKW was pre-incubated in the presence of KD-247 for 30 min at 37°C, and then PM1/CCR5 cells ($4x10^4$) were exposed to 500 $TCID_{50}$ (50% tissue culture infective dose) of the pre-incubated MOKW. After incubation for 5 h at 37°C, cells were pelleted down and resuspended in RPMI-1640 supplemented with 10% FCS without KD-247. Viral replication was monitored by observation of the cytopathic effects (CPEs) in PM1/CCR5 cells. The culture supernatant was harvested on day 7 and used to infect fresh PM1/CCR5 cells for the next round of culture in the presence of increasing concentrations of KD-247. When the virus began to propagate rapidly in the presence of KD-247, the MAb concentration was further increased. After the virus was passaged in the presence of up to 2000 μg/ml KD-247 in PM1/CCR5 cells, a KD-247-resistant virus, MOKW9p(2000), was recovered from the cell culture supernatant. MOKW was also passaged for the same time period in PM1/CCR5 cells in the absence of KD-247, and the resulting virus was designated MOKW9p(-).

Amplification of viral cDNA and nucleotide sequencing. Viral RNA was extracted from cell culture supernatants with several concentrations of KD-247 using a QIAamp viral RNA kit (Qiagen). Viral RNAs were reverse-transcribed using a High Capacity cDNA Archive Kit (Applied Biosystems) with specific antisense primer ENVN (5'-CTGCCAATCAGGGAAGTAGCCTTGTGT-3'). Nested PCR was performed to amplify the gp120 C1-C4 coding region as described previously (60). The primers used were as follows: for the first-step PCR, 1B

(5'-AGAAAGAGCAGAAGACAGTGGCAATGA-3') and H (5'-TAGTGCTTCCTGCTGCTCCCAAGAACCC-3'); for the second-step PCR, 2B (5'-AGCAGAAGACAGTGGCAATGAGAGTGA-3') and F (5'-ATATAATTCACTTCTCCAATTGTCCCTCAT-3'). The products of the nested PCR were inserted in the TA vector (Invitrogen) and sequenced using Big Dye Terminator ver.1.1 (Applied Biosystems) in accordance with the manufacturer's instructions. The sequence data from passaged samples were deposited in the DNA Data Bank of Japan under accession numbers AB262847-AB262951.

MTT assay. The neutralization-sensitivities of the each passaged MOKW viruses to KD-247 were determined as previously described (67). Briefly, PM1/CCR5 cells ($2x10^3$ cells/well) were exposed to 100 $TCID_{50}$ of each passaged virus in the presence of various concentrations of KD-247 in 96-well round-bottom microculture plates and incubated at 37°C for 7 days. After removal of 100 μl of medium from each well, 10 μl of MTT solution (7.5 mg/ml) in PBS was added to each well and the plate was incubated at 37°C for 3 h. After incubation, 100 μl of acidified isopropanol containing 4% (vol/vol) Triton X-100 was added to each well to dissolve the formazan crystals. The optical density (wavelength, 570 nm) was measured using a microplate reader. Assays were performed in duplicate or triplicate.

Construction of mutant envelope expression vectors. Proviral DNA was extracted from each batch of passaged MOKW-infected PM1/CCR5 cells using a QIAamp DNA blood mini kit (Qiagen). For the construction of each passaged envelope expression vector, we

used pCXN2, which has a chicken-actin promoter. Briefly, we amplified MOKW gp160 regions using LA *Taq* (Takara) with primers ENVA (5'-GGCTTAGGCATCTCCTATGGCAGGAAGAA-3') and ENVN (see above). The products of the PCR were inserted into pCR-XL-TOPO (Invitrogen). The sequences of the amplified *env* region of MOKW were confirmed using an ABI 377 automated DNA sequencer. The *Eco*RI fragment of pCR-XL-MOKW containing the entire *env* region was ligated into pCXN2 to give pCXN-MOKW-RDP, pCXN-MOKW-KNL/C3m and pCXN-MOKW-KNL/V3m. The pCXN-MOKW-KNL vector was constructed by replacing the *Stu*I-*Bsu*36I fragment of pCXN-MOKW-KNL/C3m with a corresponding MOKW-RDP fragment. The pCXN-MOKW-RDP/V3m and pCXN-MOKW-RDP/C3m vectors were constructed by replacing the *Stu*I-*Bsu*36I fragment of pCXN-MOKW-RDP with the corresponding pCXN-MOKW-KNL/V3m or pCXN-MOKW-KNL/C3m fragments, respectively. pCXN-MOKW-KNP, pCXN-MOKW-RDL, pCXN-MOKW-KDL and pCXN-MOKW-RNL were generated by site-directed mutagenesis using the QuickChange Site-Directed Mutagenesis Kit (Stratagene) in accordance with the manufacturer's instructions. These sequence data have been deposited in the DNA Data Bank of Japan under accession numbers AB262952-AB262961.

Pseudovirus preparation. Five μg of pNL4-3.luc.R$^-$E$^-$ and 0.5 μg of pRSV-Rev (18), supplied by the NIH AIDS Research and Reference Reagent Program, and 4.5 μg of the MOKW Env-expressing pCXN2 were cotransfected into 293T cells using the Effectene Transfection Reagent (Qiagen). At 24 h after the transfection, the pseudovirus-containing supernatants were harvested, filtered through a 0.2-μm pore-size filter and stored at –80°C.

To measure the pseudovirus activity, a luminescence assay using GHOST-hi5 cells was used as previously described (60).

Neutralization assays. A single-cycle infectivity assay was used to measure the neutralization of MOKW pseudoviruses as described previously (60). Briefly, MAb at various concentrations and a pseudovirus suspension corresponding to 100 $TCID_{50}$ were preincubated on ice for 15 min. The virus-antibody mixtures were added to GHOST-hi5 cells, which on the preceding day had been seeded in a 96-well plate ($1.5x10^4$ cells/well). Cultures were incubated for 2 days at 37°C, washed with PBS and lysed with lysis buffer (Luc PGC-50; PicaGene). Following transfer of the cell lysates to luminometer plates (Coastar 3912), the luciferase activity (in relative light units) in each well was measured using Luciferase Substrate (100 µl/well; PicaGene) in a TR717 microplate luminometer (Applied Biosystems). The reduction in infectivity was determined by comparing the relative light units in the presence and absence of MAb and was expressed as the percentage of neutralization. The same assay was repeated 2-3 times.

In vitro binding assay to the MOKW envelope-expressing cell surfaces. In vitro binding assays were performed as previously described (53, 67). *Eco*RI fragments of MOKW *env* genes from pXL-MOKWs were subcloned into the corresponding sites in pDNR-1r (Clontech). The vectors were sequenced to confirm the presence of the desired *env* gene and the absence of other changes. The *env* gene fragments were then subcloned into pLP-IRES2-EGFP (Clontech) using Cre-recombinase (Clontech) in accordance with the manufacturer's instructions. 293T cells were cotransfected with pRSV-Rev (0.5 µg) and

pLP-IRES2-EGFP-MOKW (9.5 μg) using the Effectene Transfection Reagent. After 36 h, the cells were harvested, incubated with each anti-HIV-1 MAb in combination with biotin-conjugated anti-human IgG and PerCP-conjugated streptavidin (BD Pharmingen), gated for the GFP-positive area, and analyzed using a FACSCalibur flow cytometry system.

MAb-gp120 binding assay. Culture supernatants containing the pseudotyped viruses were treated with 1% nonionic Nonidet P-40 to provide a source of gp120. Binding assays for MAbs to gp120 were then performed essentially as described elsewhere (41, 59). Briefly, gp120s from transfected culture supernatants, diluted in Tris-buffered saline containing 10% FCS and 1% Nonidet P-40, were captured onto solid phase via their carboxyl termini using sheep polyclonal antibody D7324 (Aalto Bioreagents, Dublin, Ireland). MAb was added in PBS containing 10% FCS and 0.1% nonionic detergent Tween 20, and bound MAb was detected with alkaline phosphatase-conjugated goat anti-human IgG (Sigma) followed by addition of phosphatase substrate (Sigma). A_{405} measurements were taken using a microplate reader.

Construction of chimeric NL4-3/MOKW *env* proviruses. Chimeric proviruses were constructed from the pNL4-3 proviral plasmid (AIDS Research and Reference Reagent Program, National Institute of Allergy and Infectious Diseases) by overlapping PCR as previously described with minor modifications (31). Briefly, the gp160 coding sequences were amplified from the cloning vectors using the primers EnvFv (5'-AGCAGAAGACAGTGGCAATGAGAGCGAAG-3') and EnvR (5'-TTTTGACCACTTGCCACCCATCTTATAGC-3'). A portion of the NL4-3 provirus

from nucleotides 5284 to 6232 was amplified with primers NL(5284)F (5'-GGTCAGGGAGTCTCCATAGAATGGAGG-3') and NL(6232)Rv (5'-CTTCGCTCTCATTGCCACTGTCTTCTGCT-3'). This fragment encompasses the unique *Eco*RI restriction site in pNL4-3. Another fragment from the NL4-3 provirus spanning nucleotides 8779 to 9045 was amplified using primers NL(8779)F (5'-GCTATAAGATGGGTGGCAAGTGGTCAAAA-3') and NL(9045)R (5'-GATCTACAGCTGCCTTGTAAGTCATTGGTC-3'). This fragment includes the unique *Xho*I restriction site in pNL4-3. Overlapping PCR was used to join the gp160-coding sequence from the desired clone to the fragment encompassing base 8779 to 9045 that had been amplified from pNL4-3. The resulting fragment was then similarly joined to the amplified fragment encompassing bases 5284 to 6232 from pNL4-3. The product was digested with *Eco*RI and *Xho*I and subcloned into the corresponding site in pBluescript SK(+) (Stratagene) for sequencing and subsequent manipulation. The *Eco*RI-*Xho*I fragment for each *env* gene was then subcloned back into pNL4-3. The end results were proviral plasmids that differed from each other only in the *env* gene. The resulting plasmids ware designed pNL-MOKW-RDL and pNL-MOKW-KNL.

Virus preparation and viral replication assay in PM1/CCR5 cells. Three μg of pNL-MOKW-RDL or pNL-MOKW-KNL was transfected into 293T cells using the Effectene Transfection Reagent. At 24 h after transfection, the virus-containing supernatants were harvested, filtered through a 0.2-μm pore-size filter and frozen in aliquots at –150℃. Viral yields were quantified by a RETROtek HIV-1 p24 Antigen ELISA kit (ZeptoMetrix). PM1/CCR5 cells ($1x10^4$) were exposed to NL4-3/MOKW *env* chimeric

viruses corresponding to 10ng of p24, and then pre-incubated for 4 h at 37℃. After incubation, cells were pelleted down and resuspended in RPMI-1640 supplemented with 10% FCS. Viral replication was monitored by measuring of p24 kinetics in duplicate.

ACCEPTED

Results

Anti-HIV-1 activity of KD-247 for the primary R5 isolate MOKW. KD-247 recognized an epitope that contains the IGPGR sequence located at the tip of V3 and neutralized primary HIV-1 in clade B with matching sequence motifs (11). To study how bulked primary R5 virus can escape from anti-V3 antibody, we selected a genetically heterogenous HIV-1 primary isolate, MOKW, rather than a molecular clone to allow escape mutants to be selected from a quasi-species pool as well as generated de novo. MOKW was isolated by standard PBMC culture from a drug-naïve Japanese patient infected with HIV-1 by heterosexual contact (36). The isolate was sensitive to neutralization by KD-247 with an IC_{50} of 3.4 μg/ml, which is comparable to the IC_{50} values of Ba-L, JR-FL and 89.6 (data not shown).

Selection of KD-247 escape mutants from MOKW. To select an HIV-1 variant that could escape neutralization by KD-247 in vitro, we exposed PM1/CCR5 cells to MOKW, and serially passaged the virus in the presence of increasing concentrations of KD-247. PM1/CCR5 cells were highly sensitive to both X4 and R5 HIV infection and were accompanied by prominent syncytia (68). As a control, MOKW was passaged under the same conditions but without KD-247 to allow us to monitor spontaneous changes that occurred in the virus during prolonged PM1/CCR5 cell passaging. The selected virus was initially propagated in the presence of 10 μg/ml KD-247, and during the course of the selection procedure, the MAb concentration was increased to 2000 μg/ml (Fig. 1A). After 5 rounds of passaging, a viral variant, designated MOKW5p(200), arose that replicated in the presence of 200 μg of KD-247 per ml. Moreover, after 9 rounds of passaging, a viral

variant, designated MOKW9p(2000), arose that infected PM1/CCR5 cells efficiently in the presence of 2000 μg/ml KD-247 (Fig. 1A). We harvested each passaged virus and a passaged control virus, designated MOKW9p(-), and evaluated their sensitivity to KD-247 using the MTT assay (Fig. 1B). The IC_{50} values of KD-247 against MOKW9p(-), MOKW5p(200) and MOKW9p(2000) were 0.15 μg/ml, 16 μg/ml and >100 μg/ml, respectively, indicating that MOKW had acquired a resistant phenotype against KD-247 during the in vitro selection.

Sequences of the envelope region of the KD-247 escape mutants. To determine the genetic basis underlying the resistance of the variant MOKW strains, the *env* gene was amplified and sequenced. The C1-C4 regions of the envelope were sequenced after cloning the PCR product for each region using cDNAs synthesized from viral RNAs obtained from the supernatants of infected cells as previously described (67). A total of 6-9 clones for each sample from PCR products from the passaged viruses were isolated and sequenced.

Before beginning selection by KD-247, the V2 regions of MOKW *env* had variable amino acid sequences (Fig. 2). In the first passage, two amino acid (aa) mutations in the V2 region and two aa mutations in the C3 region (5 of 9 clones) appeared, and after the 5th passage, the ratio of V2 and C3 mutated variants had further increased (7 of 8 clones). However, after the 9th passage, the C3 mutations had completely disappeared, and a Pro-to-Leu substitution (P313L) in the V3-tip emerged in addition to the mutations in the V2 region (Fig. 2). The appearance of escape mutants with a V3-tip mutation was anticipated, because prior studies on the profile of KD-247 binding to peptides suggested that amino acid substitution at the V3-tip abrogates MAb binding (11). Some changes in the

envelope sequence in other regions, including C1, V1, C2, V4 and C4, of the escape mutant were found even at early time points in the presence of the selective pressure. It is possible that these mutations also confer resistance to KD-247, but lead to viruses with decreased fitness, and thus they did not expand in the subsequent passage (Fig. 2; some data not shown). The virus passaged in PM1/CCR5 cells without KD-247 did not show the P313L substitution at passage 9 (0 of 9 clones) (Fig. 2). However, accumulation of a leucine to proline mutation at position 175 (L175P) in the V2 region was observed in the culture without KD-247. This mutation was not found in any passaged variants with KD-247.

Neutralization sensitivities of mutated MOKW pseudoviruses. To determine which substitutions were responsible for KD-247 resistance, we constructed luciferase-reporter viruses, which were pseudotyped with the representative envelopes of MOKW5p(200), MOKW9p(2000) and passaged viruses without KD-247, MOKW9p(-), and designated MOKW-KNL/C3m, MOKW-KNL/V3m and MOKW-RDP, respectively (Fig. 3). Chimeric envelopes were constructed by replacing the mutated-region (V2, V3 or C3) with a corresponding MOKW-RDP one (designed MOKW-KNL, MOKW-RDP/V3m, MOKW-RDP/C3m, respectively), and then sensitivity was compared with that of the passaged virus without KD-247. As shown in Fig. 4, the V3-tip mutated pseudoviruses, MOKW-KNL/V3m and MOKW-RDP/V3m, were completely resistant to KD-247 (>25000-fold), whereas V2 mutated viruses, MOKW-KNL/C3m and MOKW-KNL, were only partially resistant (125-fold and 500-fold respectively) (Fig. 4 and Table 1). The involvement in neutralization resistance of mutation in the V1/V2 region has been reported by number of researchers (12, 49, 50, 54). Our results show that the MOKW variants that